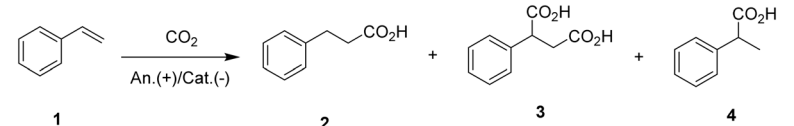


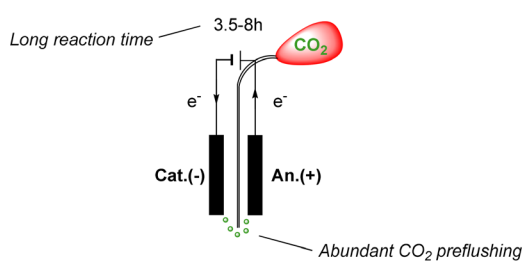
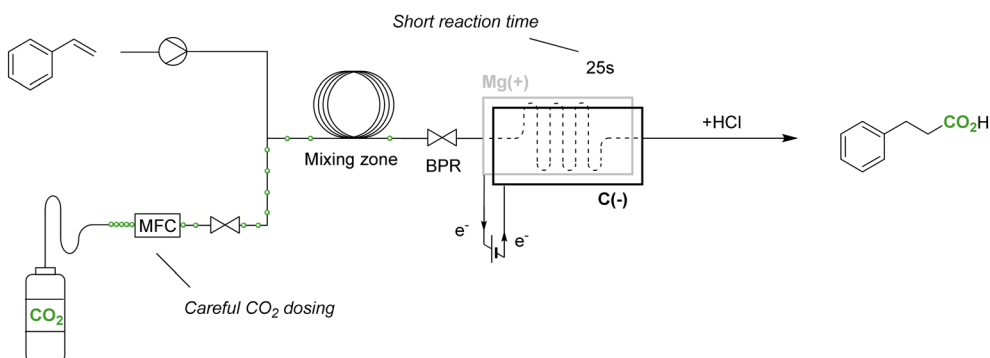
Table 1 Electrochemical carboxylation of styrene with CO₂


Ref.	Electrodes	Reaction volume	Styrene concentration	Solvent (electrolyte)	Reaction time	Conversion 1	Yield 2/3/4 (%)
12 ^a	Sm(-)/SS(+)	40 ml	0.025 M	MeCN (0.025 M Bu ₄ NPF ₆)	4 h	n.a.	65/0/0
13 ^b	C(-)/C(+)	10 ml	0.1 M	DMF (0.05 M Et ₄ NI)	3.5 h	99	62/0/8
14 ^c	Ni(-)/Mg(+)	20 ml	0.175 M	DMF (0.1 M Bu ₄ NPF ₆)	8 h	80	53/13/0

^a 10 eq. of *t*-BuOH and 8 eq. of TMSCl used in reaction. Prior to styrene addition, reaction mixture is electrolyzed for 4 hours for Sm²⁺ generation. ^b Mixture electrolyzed with a constant potential of 10 V. ^c Electrolyzed with a constant current of 35 mA, corresponding to a total charge of 3 F mol⁻¹.

the current limitations of CO₂-reductive electrochemistry. One key challenge lies in the limited selection of suitable solvents, particularly when working with species like CO₂ that require highly negative reduction potentials. Solvents with cathodic stability beyond the reduction potential of CO₂ are essential for such reactions. Suitable options include DMF, THF, and MeCN.¹⁹ Solvents with less negative cathodic limit potentials will result in competitive reactions at the working cathode, lowering the faradaic efficiency or bringing the reaction to a complete halt. Recent literature reviews reveal that DMF is predominantly utilized.^{15,20} A second limitation is the narrow choice of counter reactions. Unlike oxidative electrochemistry, which often uses simple proton reduction as the counter reaction, CO₂ reduction typically relies on

sacrificial anodes. Although literature includes examples of CO₂ reduction reactions employing non-sacrificial counter-electrodes, these approaches suffer from a poorly defined anodic chemistry and face challenges such as high operating potentials and reduced selectivity.^{12,13} Therefore, sacrificial magnesium anodes (Mg → Mg²⁺ + 2e⁻) have been chosen for the next experiments. Lastly, the widely accepted mechanism for the electrochemical carboxylation of styrene indicates that a hydrogen donor is essential for achieving β-selective hydrocarboxylation, as it ‘quenches’ the resulting radical intermediate (Fig. 2, path a). In the absence of a hydrogen donor, the reaction pathway shifts toward dicarboxylation instead^{13,21} (Fig. 2, path b). An effective hydrogen donor should have a pK_a lower than that of the corresponding

Previous work (batch)**This work (continuous flow)****Fig. 1** Advantages of continuous flow hydrocarboxylation strategy vs. batch.

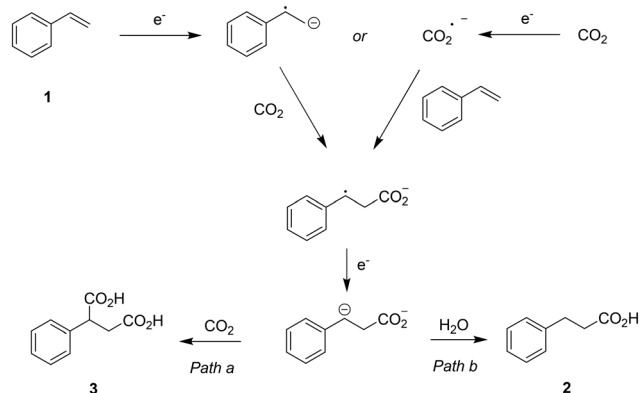


Fig. 2 Generally accepted mechanism for the electrochemical mono- and dicarboxylation of styrene at the cathode.

α -proton in the product, ensuring efficient proton transfer. At the same time, its pK_a should be high enough to minimize competitive proton reduction at the working cathode. With these criteria in mind, water ($pK_a = 14$)²² was selected as the hydrogen donor.

To analyze the hydrocarboxylation reaction in terms of electron flux, the reactor operates under constant current conditions. Maintaining a steady current, along with known reactor dimensions, (Fig. S1, ESI[†]) allows for precise calculation of the electron exposure per mole of substrate ($F \text{ mol}^{-1}$). At maximal theoretical efficiency, 2 moles of electrons are needed for every mole of substrate (Fig. 2). In practice, however, a part of the supplied electrons will lead to side reactions, e.g. unproductive proton reduction at the cathode, thus a higher electron flux is needed. The flow cell's small internal volume of 0.086 mL results in an extremely short residence time of just 25 seconds with an electron flux of $3 F \text{ mol}^{-1}$. The initial optimization was performed by saturating the reaction mixture with CO_2 bubbling, resulting in a saturated liquid reaction mixture where the CO_2 is fully dissolved. Using this pre-saturated mixture, the reaction takes place in an electrochemical flow cell driven by a syringe pump.

With all prior conditions set, an electrolyte optimization was conducted first, evaluating a group of seven candidates. Among these, Bu_4NBF_4 demonstrated the best performance (Table 2, entry 1).

As mentioned before, only DMF, MeCN and THF were considered as solvent due to their sufficiently low cathodic limit potential. When DMF was used as solvent, 86% styrene 1 was converted, yielding 68% of monocarboxylated product 2 (Table 3, entry 1). Using MeCN and THF unfortunately caused reactor clogging within just a few minutes due to fouling (Table 3, entries 2–3). When MeCN and THF were combined with DMF in equal volumes, reactor clogging could be avoided, but lower yields were obtained (Table 3, entries 4–5).

To obtain the highest yield and selectivity for β -carboxylated 2, monocarboxylation (Fig. 2, path b) needs to be favoured by adding sufficient hydrogen donor. However, the amount of hydrogen donor has an upper limit, as excessive dosing of water can lead to competitive proton reduction at the working electrode, thereby lowering the faradaic efficiency of monocarboxylated product 2 while decreasing overall conversion. An optimum was found when adding 7 eq. H_2O while running the reaction at $3 F \text{ mol}^{-1}$ (Table 4, entry 3). When adding 15 eq. H_2O , styrene conversion is significantly decreased. The presence of large gas bubbles post-reaction suggests that competitive hydrogen evolution is likely occurring—a conclusion supported by previous literature, which reported nearly 50% faradaic efficiency toward hydrogen generation upon the addition of 10 equivalents of water,²¹ ultimately leading to reduced overall conversion (Table 4, entry 4).

To promote responsible resource management, additional experiments were conducted using reduced electrolyte concentrations. Results indicated that the electrolyte concentration could be lowered from 0.1 M to 0.02 M with only a slight decrease in yield. (Table 5, entry 2) At lower concentrations, the reaction mixture lacked sufficient conductivity, causing a continuous rise in cell potential until failure (Table 5, entries 3–4).

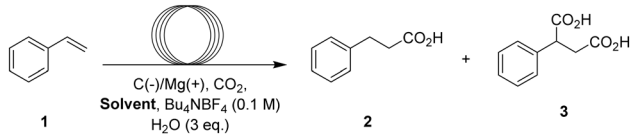
Table 2 Electrolyte screening for the electrochemical hydrocarboxylation of styrene towards 3-phenylpropionic acid

Entry ^a	Electrolyte	Conv. 1 ^b (%)	Yield 2/3 ^c (%)
1	Bu_4NBF_4	86	68/11
2	Et_4NBF_4	47	21/2
3	Me_4NBF_4	0	0
4	LiClO_4	n.d.	n.d. ^d
5	Bu_4NClO_4	81	54/14
6	Bu_4NPF_6	84	56/10
7	Et_4NI	45	22/4

^a Reactions were performed after flushing the reaction mixture with CO_2 for 30 minutes, with a styrene starting concentration of 0.05 M, under constant current conditions ($0.208 \text{ mL min}^{-1}$, 50 mA, $3 F \text{ mol}^{-1}$, 25 s residence time). ^b Conversion determined *via* quantitative HPLC analysis.

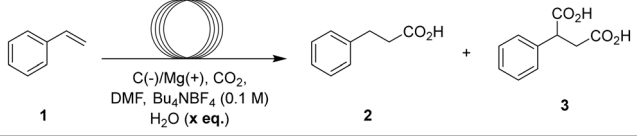
^c Yield determined *via* quantitative $^1\text{H-NMR}$ analysis of extracted products. ^d Reactor clogging, yield was not determined.



Table 3 Solvent screening for the electrochemical hydrocarboxylation of styrene towards 3-phenylpropionic acid


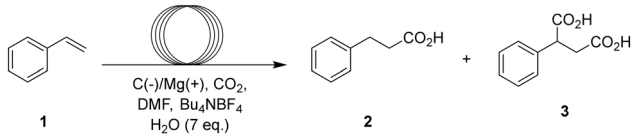
Entry ^a	Solvent	Conv. 1 ^b (%)	Yield 2/3 ^c (%)
1	DMF	86	68/11
2	MeCN	n.d.	n.d. ^d
3	THF	n.d.	n.d. ^d
4	DMF/MeCN (1/1)	75	53/9
5	DMF/THF (1/1)	78	60/8 ^e

^a Reactions were performed after flushing the reaction mixture with CO₂ for 30 minutes, with a styrene starting concentration of 0.05 M, under constant current conditions (0.208 mL min⁻¹, 50 mA, 3 F mol⁻¹, 25 s residence time). ^b Conversion determined *via* quantitative HPLC analysis. ^c Yield determined *via* quantitative ¹H-NMR analysis of extracted products. ^d Reactor clogging after a few minutes, yield was not determined. ^e Reactor started clogging near the end of the reaction.

Table 4 Hydrogen donor screening for the electrochemical hydrocarboxylation of styrene towards 3-phenylpropionic acid


Entry ^a	Hydrogen donor (eq.)	F mol ⁻¹	Conv. 1 ^b (%)	Yield 2/3 ^c (%)
1	H ₂ O (3)	3	86	68/11
		3.5	97	60/10
2	H ₂ O (5)	3	80	63/10
		3.5	89	66/11
3	H ₂ O (7)	3	87	72/10
		3.5	86	68/7
4	H ₂ O (15)	3	70	50/4
		3.5	80	58/4

^a Reactions were performed after flushing the reaction mixture with CO₂ for 30 minutes, with a styrene starting concentration of 0.05 M, under constant current conditions (for 3 F mol⁻¹: 0.208 mL min⁻¹, 50 mA, 25 s residence time. For 3.5 F mol⁻¹: 0.177 mL min⁻¹, 50 mA, 29 s residence time). ^b Conversion determined *via* quantitative HPLC analysis. ^c Yield determined *via* quantitative ¹H-NMR analysis of extracted products.

Table 5 Lowering the electrolyte concentration for the electrochemical hydrocarboxylation of styrene towards 3-phenylpropionic acid


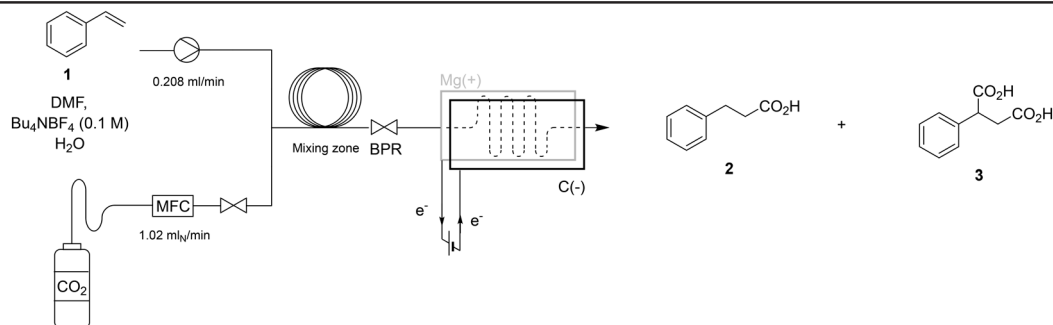
Entry ^a	Electrolyte conc.	Conv. 1 ^b (%)	Yield 2/3 ^c (%)
1	0.1 M	87	72/10
2	0.02 M	80	62/7
3	0.01 M	n.d. ^d	n.d. ^d
4	0.005 M	n.d. ^d	n.d. ^d

^a Reactions were performed after flushing the reaction mixture with CO₂ for 30 minutes, with a styrene starting concentration of 0.05 M, under constant current conditions (0.208 mL min⁻¹, 50 mA, 3 F mol⁻¹, 25 s residence time). ^b Conversion determined *via* quantitative HPLC analysis. ^c Yield determined *via* quantitative ¹H-NMR analysis of extracted products. ^d Potential gradually increased due to insufficient conductivity, thus reaching the preset safety limit of 8 V. At that point, the reaction was halted prematurely, and the yield could not be determined.

Following the initial optimization, a fully continuous flow hydrocarboxylation process was implemented, with CO₂

carefully dosed using a mass flow controller (MFC). Instead of saturating the reaction mixture with an excess of CO₂, this



Table 6 Fully continuous flow electrochemical hydrocarboxylation of styrene towards 3-phenylpropionic acid

Entry ^a	H ₂ O (eq.)	Conv. 1 ^b (%)	Yield 2/3 ^c (%)
1	1.5	84	59/3
2	3	71	56/2

^a Reactions were performed with a styrene starting concentration of 0.05 M, under constant current conditions (50 mA, 3 F mol⁻¹, 25 s residence time) with 1 bar back pressure and 4.4 eq. CO₂ (1.02 mL_N min⁻¹). ^b Conversion determined *via* quantitative HPLC analysis. ^c Yield determined *via* quantitative ¹H-NMR analysis of extracted products.

approach allows precise dosing of stoichiometric amounts, minimizing waste. To prevent leakage caused by the downstream placement of the back pressure regulator (BPR), it was relocated upstream, as the reactor is designed to operate under atmospheric pressure conditions. A homogeneous reaction stream is crucial to avoid accumulation of gas bubbles in the electrochemical cell, potentially causing fluctuations in product selectivity. *Via* trial-and-error it was observed that a maximum of 0.22 M of CO₂ could be dissolved without residual gas bubbles entering the electrolysis cell, corresponding to 4.4 equivalents of CO₂. The observed CO₂ solubility closely matches previously reported literature value.²³

In contrast to the previously identified optimum of 7 equivalents of water, the addition of just 1.5 equivalents already led to a better selectivity for monocarboxylated **2** (Table 6, entry 1 *vs.* Table 4, entry 3). Increasing the water content to 3 equivalents resulted in a noticeable decrease in conversion, suggesting that additional water offers no further benefit. (Table 6, entry 2) The reason for the overall change in product ratio compared to the syringe pump setup could not be pinpointed. A possible explanation is that residual water enters the reaction mixture, leading to a slight increase in water concentration thereby favouring formation of monocarboxylated product **2**. Despite thorough flushing of the circuit with the reaction mixture prior to the reaction, the substantial internal volume of the pump, mixing zone, and back-pressure regulator makes it challenging to completely eliminate the possibility of water contamination. Alternatively, a slightly lower CO₂ concentration is expected in this setup, operating just below the CO₂ saturation point. This reduction in CO₂ levels may, in turn, favor monocarboxylation over dicarboxylation (Fig. 2, path a *vs.* b).

Attempts to enhance productivity by increasing current were unfortunately unsuccessful, as higher currents led to the formation of a gel-like substance that clogged the reaction system (Table S1, ESI[†]). However, when maintaining the 0.05 M

substrate concentration, the electrolysis cell displayed a stable time-on-stream operation of approximately 100 residence times (Table S2, ESI[†]).

Conclusions

In summary, we have developed a convenient and fully continuous flow system for the hydrocarboxylation of styrene with CO₂, offering a highly efficient and controlled approach to this transformation. By utilizing a continuous setup, we ensure precise delivery of CO₂ in stoichiometric amounts, minimizing waste while drastically reducing the reaction time. This method not only enhances reaction efficiency but also achieves high β-selectivity and high conversion, demonstrating its potential for scalable applications.

Data availability

The data supporting this article have been included as part of the ESI[†].

Conflicts of interest

There are no conflicts to declare.

Acknowledgements

Jonas Mortier gratefully acknowledges financial support for this publication by Ghent University Special Research Fund; grant no. BOF/STA/202102/003.

Notes and references

- V. S. Pfennig, R. C. Villella, J. Nikodemus and C. Bolm, *Angew. Chem.*, 2022, **134**, e202116514.
- J. Wu, X. Yang, Z. He, X. Mao, T. A. Hatton and T. F. Jamison, *Angew. Chem., Int. Ed.*, 2014, **53**, 8416–8420.



- 3 L. Li, Z.-X. Yan, C.-K. Ran, Y. Liu, S. Zhang, T.-Y. Gao, L.-F. Dai, L.-L. Liao, J.-H. Ye and D.-G. Yu, *Chin. Chem. Lett.*, 2024, **35**, 110104.
- 4 G.-Q. Sun, W. Zhang, L.-L. Liao, L. Li, Z.-H. Nie, J.-G. Wu, Z. Zhang and D.-G. Yu, *Nat. Commun.*, 2021, **12**, 7086.
- 5 H. Seo, A. Liu and T. F. Jamison, *J. Am. Chem. Soc.*, 2017, **139**, 13969–13972.
- 6 T. Ju, Y.-Q. Zhou, K.-G. Cao, Q. Fu, J.-H. Ye, G.-Q. Sun, X.-F. Liu, L. Chen, L.-L. Liao and D.-G. Yu, *Nat. Catal.*, 2021, **4**, 304–311.
- 7 A. M. Sheta, M. A. Mashaly, S. B. Said, S. S. Elmorsy, A. V. Malkov and B. R. Buckley, *Chem. Sci.*, 2020, **11**, 9109–9114.
- 8 A. M. Sheta, A. Alkayal, M. A. Mashaly, S. B. Said, S. S. Elmorsy, A. V. Malkova and B. R. Buckley, *Angew. Chem.*, 2021, **133**, 21765–22252.
- 9 X. T. Gao, Z. Zhang, X. Wang, J. S. Tian, S. L. Xie, F. Zhou and J. Zhou, *Chem. Sci.*, 2020, **11**, 10414–10420.
- 10 B. Zhong, D. He, R. Chen, T. Gao, Y. Wang, H. Chen, Y. Zhang and D. Wang, *Phys. Chem. Chem. Phys.*, 2019, **21**, 17517–17520.
- 11 W. Zhang, L. Liao, L. Li, Y. Liu, L. Dai, G. Sun, C. Ran, J. Ye, Y. Lan and D. Yu, *Angew. Chem., Int. Ed.*, 2023, **62**, e202301892.
- 12 S. Bazzi, L. Hu, E. Schulz and M. Mellah, *Organometallics*, 2023, **42**, 1425–1431.
- 13 A. Alkayal, V. Tabas, S. Montanaro, I. A. Wright, A. V. Malkov and B. R. Buckley, *J. Am. Chem. Soc.*, 2020, **142**, 1780–1785.
- 14 N. Alhathloul, Z. Ertekin, S. Sproules and M. D. Symes, *J. Electroanal. Chem.*, 2023, **950**, 117892.
- 15 G.-Q. Sun, L.-L. Liao, C.-K. Ran, J.-H. Ye and D.-G. Yu, *Acc. Chem. Res.*, 2024, **57**, 2728–2745.
- 16 Y. Qu, C. Tsuneishi, H. Tateno, Y. Matsumura and M. Atobe, *React. Chem. Eng.*, 2017, **2**, 871–875.
- 17 S. Kumar and A. K. Singh, *Green Chem.*, 2023, **25**, 8516–8523.
- 18 A. M. Sheta, A. Alkayal, M. A. Mashaly, S. B. Said, S. S. Elmorsy, A. V. Malkov and B. R. Buckley, *Angew. Chem., Int. Ed.*, 2021, **60**, 21832–21837.
- 19 C. Schotten, T. P. Nicholls, R. A. Bourne, N. Kapur, B. N. Nguyen and C. E. Willans, *Green Chem.*, 2020, **22**, 3358–3375.
- 20 X.-F. Liu, K. Zhang, L. Tao, X.-B. Lu and W.-Z. Zhang, *Green Chem. Eng.*, 2022, **3**, 125–137.
- 21 Y. Kim, G. Do Park, M. Balamurugan, J. Seo, B. K. Min and K. T. Nam, *Adv. Sci.*, 2020, **7**, 1900137.
- 22 T. L. Neils, S. Schaertel and T. P. Silverstein, *Helv. Chim. Acta*, 2024, **107**, e202400103.
- 23 M. Jitaru, *J. Univ. Chem. Technol. Metall.*, 2007, **42**, 333–344.

